ACS APPLIED MATERIALS & INTERFACES

Letter

www.acsami.org

Boron Nitride Ultrathin Fibrous Nanonets: One-Step Synthesis and Applications for Ultrafast Adsorption for Water Treatment and Selective Filtration of Nanoparticles

Gang Lian,*[,†] Xiao Zhang,[‡] Haibin Si,[†] Jun Wang,[‡] Deliang Cui,*[,†] and Qilong Wang[‡]

[†]State Key Lab of Crystal Materials, Shandong University, Jinan 250100, P. R. China

[‡]Key Laboratory for Special Functional Aggregated Materials of Education Ministry, School of Chemistry & Chemical Engineering, Shandong University, Jinan 250100, P. R. China

Supporting Information

ABSTRACT: Novel boron nitride (BN) ultrathin fibrous networks are firstly synthesized via an one-step solvothermal process. The average diameter of BN nanofibers is only ~8 nm. This nanonets exhibit excellent performance for water treatment. The maximum adsorption capacity for methyl blue is 327.8 mg g^{-1}. Especially, they present the property of ultrafast adsorption for dye removal. Only ~1 min is enough to almost achieve the adsorption equilibrium. In addition, the BN fibrous nanonets could be applied for the size-selective separation of nanoparticles via a filtration process.

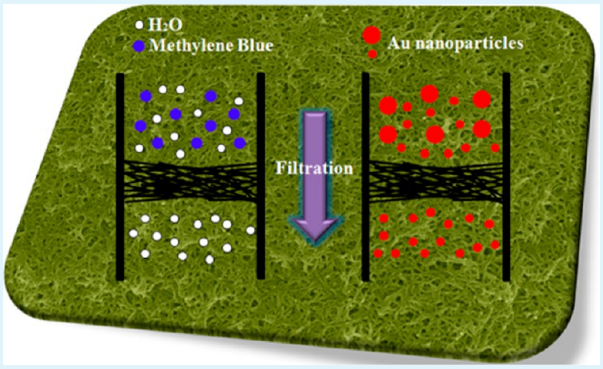

KEYWORDS: *boron nitride, fibrous nanonets, water treatment, ultrafast adsorption, selective filtration*

INTRODUCTION

The development of industry and human activity releases increasing amounts of contaminants, such as metal ions, organic dyes and cleaning agents, which has focused public concerns.[1,2] So, wastewater treatment has attracted much attention in the past decades because of grievous effluent discharge. Especially, some dyes discharged from plating, textile, and printing industries are resistant to diological degradation, which is quite difficult to remove from the wastewater.[3,4] Among the various technologies (such as photocatalytic degradation,[5] electrochemical degradation,[6] and adsorption[7,8]), adsorption is considered one of the most efficient and economical methods for water purification.[9] Then many polymetic and inorganic adsorbents have been developed, such as carbonaceous nanomaterials,[10] porous metal oxides,[11] clays,[12] chitosan,[13] and zeolites.[14] However, they frequently suffer from the disadvantage of limited adsorption capacity or slow adsorption rate, which is generally limited by less adsorption sites, slow kinetics and nonequilibrium of adsorption.[15] Therefore, it is necessary to develop new adsorbents with high adsorption capacity and ultrafast adsorption characteristic.

Currently, various nanostructures have been applied for removal of pollutants from wastewater, including hollow spheres,[16] nanoflowers,[17] nanofibers,[18] nanonets[19] and so on. Nanofiber network is one of the most promising adsorption structures. Because of their high surface-to-volume ratio, high porosity, and interconnected open pores, it can remarkably enhance the physical and chemical adsorption. Su et al reported the $W_{18}O_{49}$ nanowire networks with superior performance for adsorption of MB, RhB and Pb(II).[19] Xiong et al fabricated a mesoporous NiO ultrathin nanowire networks, which also presented excellent capacity on the adsorption of Congo red.[20]

Boron nitride (BN) is isostructural to graphite and has received considerable attention due to its wide band gap, high thermal conductivity, excellent oxidation resistance and good chemical inertness.[21−24] In the last decade, a lot of investigations have been concentrated on the preparation of various BN nanostructures, such as nanoparticles,[25] nanotubes,[26] nanofibers,[27] nanoribbons,[28] nanosheets,[29] hollow spheres,[16] nanoflowers,[30] etc. Among them, ultrathin fibrous nanonets possibly indicate excellent performance on adsorption and filtration because of large specific surface area, high surface-to-volume ratio and interconnected open pores. However, the efficient synthesis of BN nanofiber networks, especially ultrathin fibrous nanonets, still remains a challenge. As we know, this special microstructure has never been reported so far. Herein, we present an original strategy to fabricate novel BN ultrathin nanofiber network via a solvothermal process. The synthesis of BN following the reaction of NH_4BF_4 and NaN_3 was conducted at at 260 °C with an assistance of CS_2. In the

Received: September 4, 2013
Accepted: November 27, 2013
Published: November 27, 2013

reaction process, NH_4N_3 gas, as a very important intermediate (see Figure S1 in the Supporting Information), firstly formed with the increase in temperature and then rapidly diffused into the liquid medium (Scheme 1a). Secondly, the fresh $NaBF_4$ would decomposed to generate BF_3 gas (Scheme 1b). Then a convective diffusion of gaseous NH_4N_4 and BF_3 species would induce the formation of BN nano-fragment in the reaction medium. Because of the convective diffusion was precisely conducted along the vertical direction, the fresh BN fragment would easily stacked to form fibrous nanostructure. It was reported that CS_2 could induce the fast decomposition of azides,[31] which possibly promoted the formation of smaller BN nano-fragment by improving the reaction activity of NH_4N_3. As a result, ultrathin BN nanofibers (Scheme 1c) were obtained with the assistance of CS_2. However, the BN nanofibers were too thin to vertically stand into an array shape. They then naturally fell down and formed porous nanonet via connecting with each other (Scheme 1d).

Scheme 1. Schematic Illustration of the Formation Process of BN Ultrathin Fibrous Nanonets

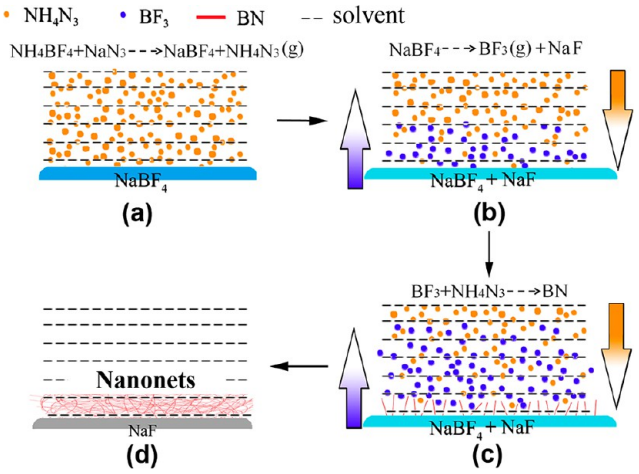

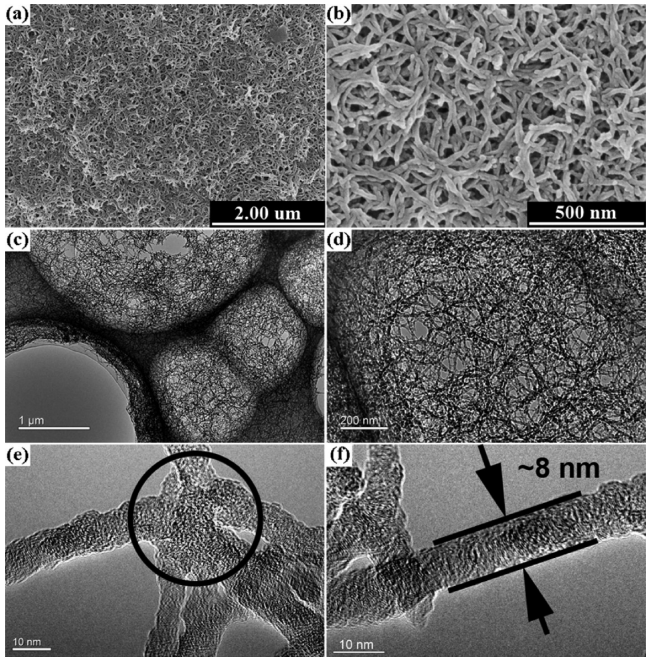

Figure 1. BN ultrathin fibrous nanonets prepared by one-step solvothermal process with CS2 as the catalysts. (a, b) Typical SEM images and (c, d) the corresponding TEM images of BN nanonet with different magnification ratios; (e, f) HRTEM images of a typical fibrous knot (circled) and a BN nanofiber with diameter of ~8 nm.

RESULTS AND DISCUSSION

The phase structure of as-obtained sample is firstly confirmed by the XRD pattern (see Figure S2 in the Supporting Information). The reflection peaks at ~26 and ~42° can be indexed to the (002) and (100) planes of hBN, respectively. In the FTIR spectrum (see Figure S3 in the Supporting Information), besides the peak of adsorbed water at 3418 cm^{-1}, only two obvious peaks, at 1410 and 780 cm^{-1} are observed. They are attributed to ν(B−N) and δ(B−N−B) modes of hBN, respectively.

Images a and b in Figure 1 show the typical BN nanofiber network prepared with 50 μL of CS_2 as the catalyst, in which a large amount of uniform BN nanofibers are cross-linked with each other. Meanwhile, the cross-linked nanofibers form a nanonet structure with high porosity on the rough surface. Furthermore, the TEM images shown c and d in Figure 1 indicate that the 2D nanonet is completely constructed by BN ultrathin nanofibers, and a large amount of interconnected open nanopores are clearly observed. These open nanopores make the convection mass exchange within these nanonets happen easily, thus rapid adsorption characteristic and selective sieving performance can be expected. Besides, differing from the conventional solvent-evaporation-induced self-assembly process, the as-obtained BN network was formed by BN ultrathin nanofibers interconnected via a large amount of "knots", rather than a simple accumulation process (Figure 1d, e). A typical knot is shown in Figure 1e, which is formed by several BN nanofibers with average diameter of ~8 nm (Figure 1f and Figure S4 in the Supporting Information). The ultrathin BN nanofibers can supply much more active adsorption sites and should exhibit higher adsorption efficiency.

In addition, a group of comparative experiments showed that suitable content of CS_2 catalyst contributed to the formation of BN ultrathin nanofiber networks. In the reaction system without CS_2 added, only BN nanorods with an average diameter of ~50 nm were obtained (see Figure S5a in the Supporting Information). When 15 μL of CS_2 were employed, a large amount of BN nanofibers were fabricated (see Figure S5b in the Supporting Information). The average diameter of these nanofibers is ~25 nm, but they could not assembly into netlike nanostructure.

The nitrogen-sorption isotherm was measured to illustrate the specific surface area (SSA) and pore volume of the BN ultrathin fibrous nanonets (see Figure S6 in the Supporting Information). They exhibit type IV isotherm with a H1 hysteresis loop, implying the mesoporous structure. The BET SSA and BJH pore volume were evaluated to 114.5 $m^2\ g^{-1}$ and 0.37 $cm^3\ g^{-1}$. The pore volume is mainly attributed to the network structure.

To explore the adsorption and filtration performances of BN nanonets, firstly, its contact angle (CA) and zeta-potential were measured to study the water wettability. The CA measurement result indicates that BN nanonet exhibits well hydrophilic (Figure 2a). Because a large number of dangling bonds expose on the external surface of ultrathin nanofibers, the water molecules easily adsorb on them. This process thus results in the formation of abundant −OH to terminate these dangling

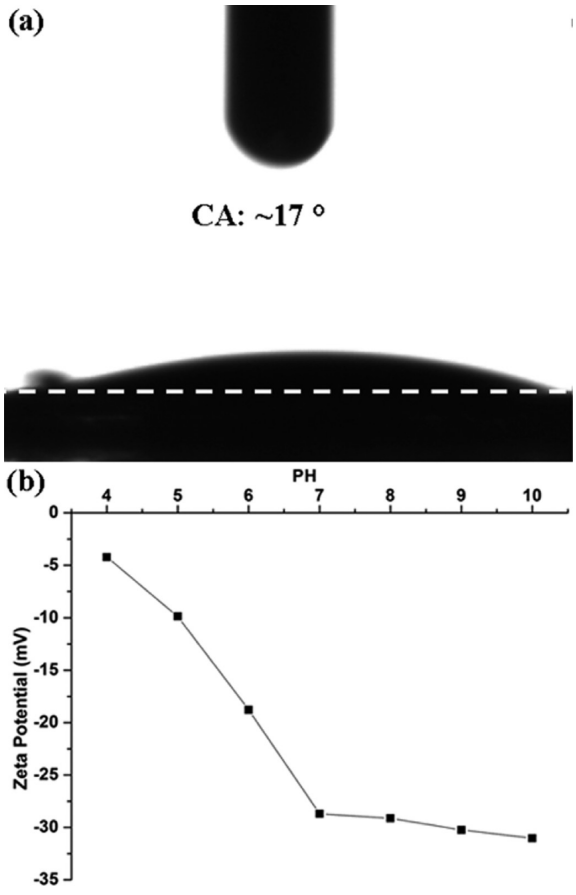

Figure 2. (a) Water contact angle (CA) on the BN nanonet; (b) Zeta potential vs. pH value of the BN nanonet.

bonds, which were identified by the FTIR spectrum (see Figure S3 in the Supporting Inforamtion). The functional groups not only facilitate superior sorption, but also increase the hydrophilicity. The Zeta-potential result shows that the nanonet sample has an overall negative surface charge at above pH 4 (Figure 2b). The zeta potential decreases towards acidic PH values. The low isoelectric point is an indication of abundant acidic sites on BN nanonet. The functional group (−OH) on the surface of BN nanonet is responsible for the surface negative charge, which plays a key role in retaining the contaminants via electrostatic adsorption process.

The adsorption kinetic test of BN nanonet was conducted to evaluate its adsorption rate of pollutants from the wastewater. Herein, methylene blue (MB) was chosen as the indicant reagent for examining the adsorption performance. To directly observe the quick removal of pollutants by the BN nanonet, 5 mg of sample was added to 10 mL of MB solution with an initial concentration of 20 mg L^{-1}. Figure 3a shows that the color of MB solution almost disappeared within 10 s, i.e., more than 98 % of MB was quickly removed from the solution. Furthermore, to illustrate the quick adsorption nature of the nanonet, the ratios of residual MB concentrations to initial one at different time intervals were recorded after 5 mg of BN product was added into 10 mL of MB solution with an initial concentration of 200 mg L^{-1} (Figure 3b). About 51.3 % of MB was removed after the sample was added into the solution for 1 min, whereas only ~3.6 % additional MB was removed after the next ~120 min adsorption. The equilibrium adsorption capacity was 219.6 mg g^{-1}. In other words, the adsorption equilibrium can be almost achieved in very short time, which is significantly faster than that of commerical active carbon and some traditional nanostructures. The ultrafast removal rate in the beginning 1 min was attributed to the rapid diffusion and strong electrostatic interaction of MB from the solution to the external surfaces of BN nanonets.

The adsorption capacity at different equilibrium concentrations is shown in Fig. 3c. The Langmuir isotherm model was employed to describe the relationship between the equilibrium adsorption capacity (q_e, mg g^{-1}) and its equilibrium solute concentration (C_e, mg L^{-1}).[32] The linear form of Langmuir isotherm is expressed by eq 1

$$C_e/q_e = 1/q_m b + C_e/q_m \quad (1)$$

where q_m (mg g^{-1}) is the maximum adsorption capacity corresponding to complete monolayer coverage, and b is the equilibrium constant. The Langmuir isotherm for MB adsorption on BN nanonet is shown in Figure S7 in the Supporting Information. The experimental data fit the Langmuir adsorption isotherm well. The maximum adsorption capacity of BN nanonet for MB was as high as 327.8 mg g^{-1}, which is close to the maximum adsorption capacity of 296.7 mgg^{-1} with the initial concentration of 350 mg L^{-1} (see Figure S8in the Supporting Information). Moreover, when the initial concentration of MB increased from 20 to 350 mg L^{-1}, the removal percentage of MB decreased from 99.2 to 42.2 %. So, the removal efficiency of MB decreased with an increase in initial MB concentration. The high adsorption capacity and ultrafast removal percentage make the BN nanonet efficient in wastewater treatment. In addition, the kinetic of adsorption is an important characteristic defining the adsorption efficiency. Herein, pseudo-second-order model (eq 2) was tested to investigate the adsorption mechanism.[33]

$$t/q_t = 1/k_2 q_e^{\,2} + t/q_e \quad (2)$$

where q_t is the adsorption capacity at time t (min) and k_2 (g mg^{-1} min^{-1}) is the rate constant of pseudo second order model. As shown in Figure 3d and Figure S9 in the Supporting Information, The experimental data fit the pseudo second order model well on the basis of the correlation coefficient (R^2). The q_e value of 218.3 mg g^{-1} calculated with this model was very close to the experimental value (219.6 mg g^{-1} from Figure 3b). This indicates that the rate-limiting step was a chemcial adsorption process between the adsorbate and adsorbent.[34]

Then a simple experiment was conducted to intuitively verify the ultrafast adsorption process. First, 20 mg of BN nanonet sample was dispersed into 5 mL of ethanol by vigorously stirring for several hours. The obtained suspension was then casted into a filter funnel. After dried at ambient temperature, an analogous filtration membrane obtained. Finally, 5 mL of MB solution with a concentration of 200 mg L^{-1} flowed through the filtrated membrane, as shown in Figure 3e. After a few seconds, colorless water was obtained by filtrating the deep blue MB solution with a flow rate of ~2.5 mL min^{-1}. The result indicates that the MB species were completely adsorbed by the BN nanonet sample (Figure 3f). The absorption spectra correspond to an original (i: 10 mg L^{-1}, which is obtained by diluting the concentration of 200 mg L^{-1} to its 1/20 degree) and filtration-treated (ii) MB solutions, respectively.

Except for the adsorption filtration of pollutant wastewater (Figure 3e), the BN nanonet membrane can be also used as nanomesh for separating nanoparticles with different particle

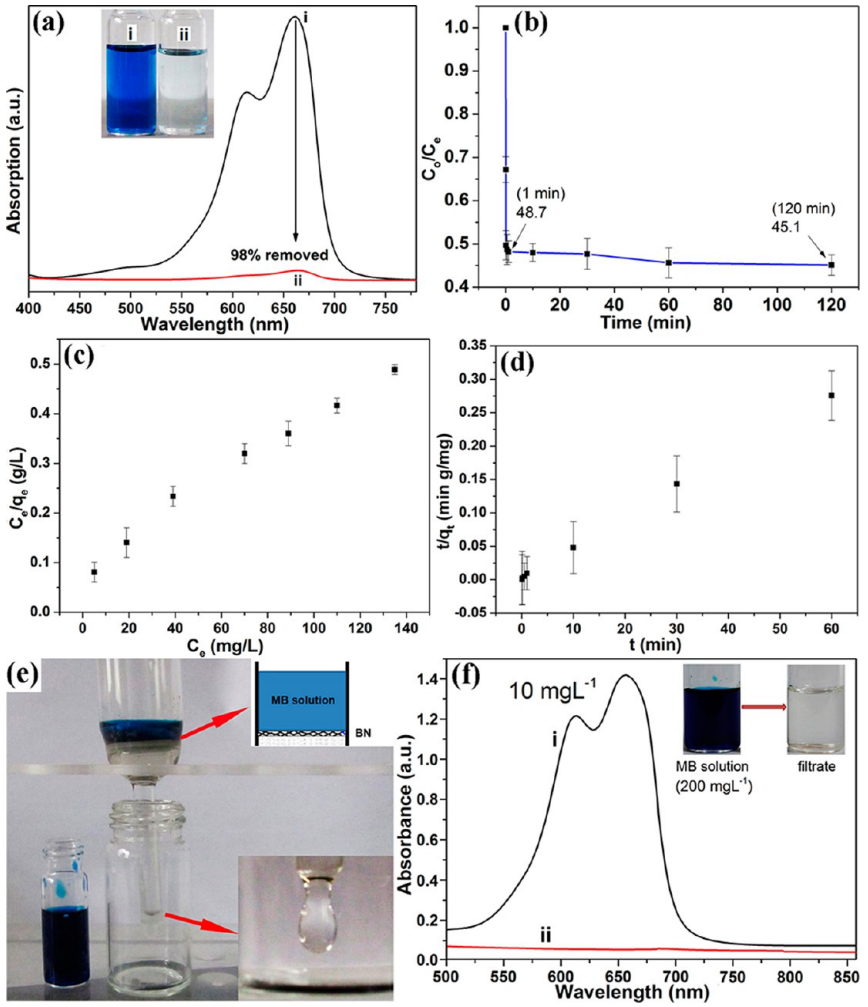

Figure 3. (a) Absorption spectra of the (i) original (20 mg L^{-1}) and (ii) adsorbing-treated MB solutions. The MB solution was treated by adding 5 mg of BN nanonet into 10 mL of MB solution. Inset: photograph of the original and treated solutions. (b) Adsorption rate curve of MB on BN nanonets. The adsorption rate test was conducted with an initial MB concentration of 200 mg L^{-1}; (c) adsorption capacities at different equilibrium concentrations; (d) the adsorption capacities at different time intervals; (e) photograph shows the filtration performance of BN nanonet membrane for MB solution; (f) corresponding absorption spectra of the (i) original (10 mg L^{-1}) and (ii) filtration-treated MB solutions.

sizes. Herein, two kinds of Au nanoparticles with average particle sizes of 15 and 34 nm (see Figure S10 in the Supporting Information) were selected for examining the sieving performance of BN nanonet membrane. Just as indicated by Figure 4, ~90 % of the 15 nm Au nanoparticles can freely pass through the nanonet membrane, which was calculated from the adsorption intensities at 519 nm (Figure 4a). In a sharp contrast, almost all the 34 nm Au nanoparticles (adsorption intensity at 526 nm) have been filtered out from the solution, as shown in Figure 4b. The top surface of the BN nanonet membrane before and after sieving the 34 nm Au nanoparticles further confirm that it is an effective nanomesh for separating nanoparticles according to their sizes (Figure 4c, d). On the basis of the permeability property of the nanonet membrane studied above, we attempted to use it for the separation of Au nanoparticles from the binary mixture (15/34 nm). First, when the two kinds of Au nanoparticle solutions were mixed together with a same volume, a new broad adsorption peak appeared at 523 nm instead of two individual peaks at 519 and 526 nm, respectively. Then, the mixture was filtered through the membrane. After filtration, the adsorption peak at 519 nm appeared again, which could illuminate that the membrane rejected most of the 34 nm particles and allowed the 15 nm particles to pass freely (see Figure S11 in the Supporting Information).

CONCLUSIONS

In summary, we first report a novel BN ultrathin nanofiber networks prepared by one-step solvothermal process. Suitable content of CS_2 catalyst in the reaction system has a significant effect on the formation of net-like nanostructure. The average diameter of BN nanofibers is only ~8 nm, which is the thinnest up to now. They exhibit the maximum adsorption capacity of 327.8 mgg^{-1} for MB. More importantly, they present excellent ultrafast adsorption characteristic for the organic dye. Only ~1 min is enough to almost achieve the adsorption equilibrium. The high adsorption capacity and ultrafast adsorption characteristic make it a potentially attractive adsorbent in water purification. In addition, a filtration membrane consisting of these nanonets also displays a sieving performance for nanoparticles with different sizes via a filtration process.

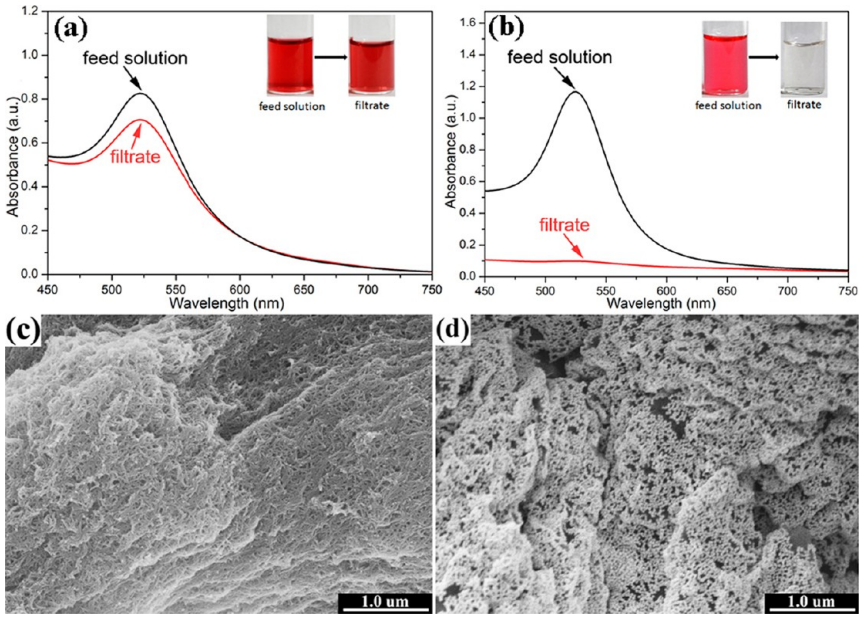

Figure 4. UV−vis spectra of the feed and filtrate Au nanoparticles solutions, which exhibit the sieving performance of BN nanonet membrane. (a) Filtration of 15 nm Au nanoparticles; (b) filtration of 34 nm Au nanoparticles. (c, d) SEM images of BN nanonet membrane (a) before and (b) after filtration of 34 nm Au nanoparticles.

■ ASSOCIATED CONTENT

Supporting Information

Detailed experimental procedures, a photo and FTIR spectra of intermediate NH_4N_3, XRD pattern and FTIR spectrum of BN, the TEM images and diameter distribution of BN ultrathin nanofibers, BN nanorods and nanofibers synthesized with different contents of CS_2 additives, nitrogen-sorption isotherm and pore diameter distribution of BN ultrathin nanofiber nanonets, and the TEM images of Au nanoparticles with average diameter of 15 and 34 nm. This material is available free of charge via the Internet at http://pubs.acs.org.

■ AUTHOR INFORMATION

Corresponding Authors

*E-mail: cuidl@sdu.edu.cn. Phone: (+86)-531-88361856. Fax: (+86)-531-88361856.
*E-mail: liangang@sdu.edu.cn

Notes

The authors declare no competing financial interest.

■ ACKNOWLEDGMENTS

The authors express our faithful thanks to Prof. Haibing Xia, Dr. Jihui Zhang, and Peina Zhang for their kindly help in preparing Au nanoparticles. This work was supported by the Natural Science Foundation of China (NSFC 50990061, 21073107, 51102151, 51372143), Natural Science Foundation of Shandong Province (ZR2011EMQ002), and Independent Innovation Foundation of Shandong University (2012GN051).

■ REFERENCES

(1) Kaur, S.; Gopal, R.; Ng, W. J.; Ramakrishna, S.; Matsuura, T. *MRS Bull.* **2008**, *33*, 21−26.
(2) Liang, H. W.; Cao, X.; Zhang, W. J.; Lin, H. T.; Zhou, F.; Chen, L. F.; Yu, S. H. *Adv. Funct. Mater.* **2011**, *21*, 3851−3858.
(3) Zhong, L. S.; Hu, J. S.; Liang, H. P.; Cao, A. M.; Song, W. G.; Wan, L. J. *Adv. Mater.* **2006**, *18*, 2426−2431.
(4) Zimmerman, J. B.; Mihelcic, J. R.; James, S. *Environ. Sci. Technol.* **2008**, *42*, 4247−4254.
(5) Xiong, Z.; Zhang, L. L.; Ma, J.; Zhao, X. S. *Chem. Commun.* **2010**, *46*, 6099−6101.
(6) Prakash, S.; Rajesh, A. M.; Shahi, V. K. *Chem. Eng. J.* **2011**, *168*, 108−114.
(7) Ai, L.; Yue, H.; Jiang, J. *Nanoscale* **2012**, *4*, 5401−5408.
(8) Wang, B.; Wu, H.; Yu, L.; Xu, R.; Lim, T. T.; Lou, X. W. *Adv. Mater.* **2012**, *24*, 1111−1116.
(9) Crittenden, J. C.; Trussell, R. R.; Hand, D. W.; Howe, K. J.; Tchobanoglous, G. In *Water Treatment: Principles and Design*, 2nd ed.; Wiley: Chichester, U.K., 2005; Chapter 4, p 165.
(10) Xu, Y. J.; Weinberg, G.; Liu, X.; Timpe, O.; Schlogl, R.; Su, D. S. *Adv. Funct. Mater.* **2008**, *18*, 3613−3619.
(11) Zhu, T.; Chen, J. S.; Lou, X. W. *J. Phys. Chem. C* **2012**, *116*, 6873−6878.
(12) Valix, M.; Cheung, W. H.; Mckay, G. *Langmuir* **2006**, *22*, 4574−4582.
(13) Lazaridis, N. K.; Kyzas, G. Z.; Vassiliou, A. A.; Bikiaris, D. N. *Langmuir* **2007**, *23*, 7634−7643.
(14) Alvarez-Ayuso, E.; Garcia-Sanchez, A.; Querol, X. *Water Res.* **2003**, *37*, 4855−4862.
(15) Mauter, M. S.; Elimelech, M. *Environ. Sci. Technol.* **2008**, *42*, 5843−5859.
(16) Lian, G.; Zhang, X.; Zhang, S. J.; Liu, D.; Cui, D. L.; Wang, Q. L. *Energy Environ. Sci.* **2012**, *5*, 7072−7080.
(17) Jeon, S. H.; Yong, K. J. *J. Mater. Chem.* **2010**, *20*, 10146−10151.
(18) Lu, X. H.; Zheng, D. Z.; Gan, J. Y.; Liu, Z. Q.; Liang, C. L.; Liu, P.; Tong, Y. X. *J. Mater. Chem.* **2010**, *20*, 7118−7122.
(19) Gao, X. Q.; Xiao, F.; Yang, C.; Wang, J. D.; Su, X. T. *J. Mater. Chem. A* **2013**, *1*, 5831−5834.
(20) Li, X. W.; Xiong, S. L.; Li, J. F.; Bai, J.; Qian, Y. T. *J. Mater. Chem.* **2012**, *22*, 14276−14283.
(21) Wu, J.; Han, W. Q.; Walukiewicz, W.; Ager, J. W., III; Shan, W.; Haller, E. E.; Zettl, A. *Nano Lett.* **2004**, *4*, 647−650.
(22) Watanabe, K.; Taniguchi, T.; Kanda, H. *Nat. Mater.* **2004**, *3*, 404−409.
(23) Kubota, Y.; Watanabe, K.; Tsuda, O.; Taniguchi, T. *Science* **2007**, *317*, 932−934.

(24) Macnaughton, J. B.; Moewes, A.; Wilks, R. G.; Zhou, X. T.; Sham, T. K.; Taniguchi, T.; Watanabe, K.; Chan, C. Y.; Zhang, W. J.; Bello, I.; Lee, S. T. *Phys. Rev. B* **2005**, *72*, 195113.
(25) Tang, C. C.; Bando, Y.; Huang, Y.; Zhi, C. Y.; Golberg, D. *Adv. Funct. Mater.* **2008**, *18*, 3653−3661.
(26) Tokoro, H.; Fujii, S.; Oku, T. *Mater. Chem. Phys.* **2009**, *114*, 204−212.
(27) Qiu, Y. J.; Yu, J.; Rafique, J.; Yin, J.; Bai, X. D.; Wang, E. G. *J. Phys. Chem. C* **2009**, *113*, 11228−11234.
(28) Chen, Z. G.; Zou, J.; Liu, G.; Li, F.; Wang, Y.; Wang, L. Z.; Yuan, X. L.; Sekiguchi, T.; Cheng, H. M.; Lu, G. Q. *ACS Nano* **2008**, *2*, 2183−2191.
(29) Zhi, C. Y.; Bando, Y.; Tang, C. C.; Kuwahara, H.; Golberg, D. *Adv. Mater.* **2009**, *21*, 2889−2893.
(30) Lian, G.; Zhang, X.; Tan, M.; Zhang, S. J.; Cui, D. L.; Wang, Q. L. *J. Mater. Chem.* **2011**, *21*, 9201−9207.
(31) Feigl, F.; Anger, V. In *Spot Tests in Organic Analysis*, 7th ed.; Butterworth Heinemann: Oxford, U.K., 1966; Chapter 6, p 587.
(32) Langmuir, I. *J. Am. Chem. Soc.* **1918**, *40*, 1361−1403.
(33) Ho, Y. S. *J. Hazard. Mater.* **2006**, *136*, 681−689.
(34) Wu, F. C.; Tseng, R. L.; Huang, S. C.; Juang, R. S. *Chem. Eng. J.* **2009**, *151*, 1−9.